Electron Scattering: Form Factors and Nuclear Shapes

Kyle Foster

November 16, 2011

1 Brief History of Early Electron Scattering Experiments

- 1951 Early electron scattering experiments are performed at University of Illinois. A 15.7 MeV beam allows for confirmation of Rutherford's earlier approximation $R \sim 10^{-13} A^{1/3}$
- 1953 Standford and Michigan have electron beams running at energies up to 190 MeV. Lots of new experimental data becomes available
- 1961 Robert Hofstadter wins Nobel Prize for 'his pioneering studies of electron scattering in atomic nuclei and for his thereby achieved discoveries concerning the structure of the nucleons'

2 Form Factors from Scattering Experiments

Form Factors are an intuitive and simple tool used to describe the scattering particles from extended targets. Here we will show how the Form Factor comes about in the context of the scattering of spinless electrons. A discussion of the more rigorous descriprtion, which includes electron spin a magentic moment, will follow.

The basic experimental approach is consistant with what has already been discussed in the course: The typical set up has an electron beam with initial

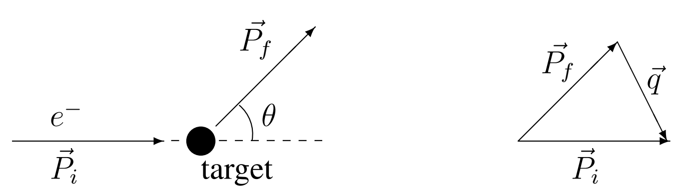

momentum $\vec{P}_i$ directed at the scattering target. The electrons are deflected through an angle θ with a final momentum $\vec{P}_f$.We define the momentum transfer as the vector $\vec{q} = \vec{P}_i - \vec{P}_f$.

As with many scattering experiments, the quantity we are interested in is the differential cross section $\frac{d\sigma}{d\Omega}$ of our scattered electrons off our target. This quantity can be measured in the lab and easily connected to QM scattering theory in order to confirm theory and provide insight to the physical processes at play.

Earlier we had shown that the differential cross section is related to the scattering amplitudes through the relation:

$$\frac{d\sigma}{d\Omega} = \frac{k}{k_i}|f(\theta,\phi)|^2 \tag{1}$$

The scattering amplitudes $f(\theta,\phi)$ can be obtained in approximate form using the Born Approximation. To first order (and up to a normalization) the Born Approximation can be written as:

$$f_{B1} = \left\langle \phi_{\vec{k_f}} \right| V \left| \phi_{\vec{k_i}} \right\rangle \tag{2}$$

$$= \int \phi^*_{\vec{k_f}}(\vec{r})V(\vec{r})\phi_{\vec{k_i}}(\vec{r})d^3\vec{r} \tag{3}$$

In the first Born Approximation the initial incoming wave and the outgoing waves are assumed to be plane waves of the form:

$$\phi_{\vec{k_i}}(\vec{r}) = e^{i\vec{k_i}\cdot\vec{r}} \tag{4}$$

$$\phi_{\vec{k_f}}(\vec{r}) = e^{i\vec{k_f}\cdot\vec{r}} \tag{5}$$

We will also define the momentum transfer as $\frac{\vec{q}}{\hbar} = \vec{k_i} - \vec{k_f}$. Making use of these deinitions the first Born Approximation can be written as:

$$f_{B1} = \int e^{\frac{i\vec{q}\cdot\vec{r}}{\hbar}} V(\vec{r})d^3\vec{r} \tag{6}$$

This result is still quite general; in order to proceed we will need to assume a specific form for the potential, $V(\vec{r})$. We can describe an extended charge distribution by $Ze\rho(\vec{r})$ with

$$\int \rho(\vec{r})d^3\vec{r} = 1 \tag{7}$$

In this case, the potential experienced by an electron located at $\vec{r}$ is given by the Coloumb potential:

$$V(\vec{r}) = \frac{-Ze^2}{4\pi\epsilon_0}\int \frac{\rho(\vec{r}')}{|\vec{r}-\vec{r}'|}d^3\vec{r}' \tag{8}$$

Substitue this potential into the general expression for the first Born Approximation to the scattering amplitudes $f(\theta, \phi)$ (eq. 6)

$$f_{B1} = \frac{-Ze^2}{4\pi\epsilon_0} \int e^{\frac{i\ q \cdot \vec{r}}{\hbar}} \int \frac{\rho(\vec{r}')}{|\vec{r} - \vec{r}'|} d^3\vec{r}' d^3\vec{r} \tag{9}$$

Make the substitution $\vec{R} = \vec{r} - \vec{r}'$ and noting that $d^3\vec{R} = d^3\vec{r}$,

$$f_{B1} = \frac{-Ze^2}{4\pi\epsilon_0} \int e^{\frac{i\vec{q}\cdot\vec{R}}{\hbar}} \int \frac{e^{\frac{i\vec{q}\cdot\vec{r}'}{\hbar}} \rho(\vec{r}')}{|\vec{R}|} d^3\vec{r}' d^3\vec{R} \tag{10}$$

$$= \frac{-Ze^2}{4\pi\epsilon_0} \int \frac{e^{\frac{i\vec{q}\cdot\vec{R}}{\hbar}}}{|\vec{R}|} d^3\vec{R} \left[\int e^{\frac{i\vec{q}\cdot\vec{r}'}{\hbar}} \rho(\vec{r}') d^3\vec{r}' \right] \tag{11}$$

This bracked factor is known as the 'Form Factor', $F(q)$.

$$F(q) = \int e^{\frac{i\vec{q}\cdot\vec{r}'}{\hbar}} \rho(\vec{r}') d^3\vec{r}' \tag{12}$$

It can be shown that when the expression for f_{B1} is used to determine $\frac{d\sigma}{d\Omega}$, that:

$$\frac{d\sigma}{d\Omega} = \left(\frac{Ze^2}{4E} \right) \frac{1}{\sin^4(\frac{1}{2}\theta)} |F(q)|^2 \tag{13}$$

This expression can be interpreted intuitively as Rutherford scattering modulated by the square of the Form Factor. In other words, electron scattering off an extended source is equal to scattering off a point source modulated by the form factor.

A rigourous treatment of the problem of electron scattering, with consideration of electron spin and magnetic moment (with no spin or magentic moment assumed for the target), was first accomplished by Mott in 1929. The so-called Mott cross section for electron scattering from a point charge is given by:

$$\frac{d\sigma}{d\Omega} = \left(\frac{Ze^2}{2E} \right) \frac{\cos^2(\frac{1}{2}\theta)}{\sin^4(\frac{1}{2}\theta)} \tag{14}$$

This equation is true under a couple assumptions. First, the energy of the electron must be such that $\beta \approx 1$ so that β^4 can safely be set to unity. This is a good approximation (within 0.5%) for electron energies greater than 10 MeV.

The second assumption is that the target is comprised of light nuclei as defined by $\frac{Z}{137} = \frac{Ze^2}{\hbar c} \ll 1$. This a reasonable assumption for elements up to around Calcium.

The form of this differential cross section bears a striking resemblence to that of Rutherford scattering, the only difference being a factor of $4\cos^2(\frac{1}{2}\theta)$. If an extended charge distribution is considered as the scattering target, the Mott cross section becomes:

$$\frac{d\sigma}{d\Omega} = \left(\frac{Ze^2}{2E}\right)\frac{\cos^2(\frac{1}{2}\theta)}{\sin^4(\frac{1}{2}\theta)}|F(q)|^2 \tag{15}$$

Analogous to the spinless electron treatment.

3 Form Factors

The form factor was defined in eq. 12 as:

$$F(q) = \int e^{\frac{i\vec{q}\cdot\vec{r}'}{\hbar}}\rho(\vec{r}')d^3\vec{r}' \tag{16}$$

Upon inspection this equation can be idenitfied as the Fourier transform of the spatial charge distribution, $\rho(\vec{r}')$. This provides a powerful tool for determining the spatial charge distribtuions of the nuclei resonsible for the scattering.

The special case of a spherically symmetric charge distribution can be easily analyzed. In the case of spherical symmetry (and spherical coordinates) we have:

$$\rho(\vec{r}') = \rho(r') \tag{17}$$

$$d^3\vec{r}' = r'^2 d(\cos(\theta))d\phi dr' \tag{18}$$

And so eq. 16 can be written as:

$$F(q) = \int_0^{2\pi} d\phi \int_{-1}^{-1} d\cos(\theta) \int_0^{\infty} e^{\frac{iqr\cos(\theta)}{\hbar}}\rho(r')dr' \tag{19}$$

$$= 2\pi \int_0^{\infty}\left[\frac{\hbar}{iqr'}e^{\frac{iqr\cos(\theta)}{\hbar}}\right]_{-1}^{1} r'^2\rho(r')dr' \tag{20}$$

$$= 4\pi \int_0^{\infty}\frac{\sin(qr'/\hbar)}{qr'/\hbar}r'^2\rho(r')dr' \tag{21}$$

This tidy expression is a useful form of the Form Factor given the typical experimental setup and the widespread use of the spherically symmetric assumption.

Furthermore, one can define a root-mean-square radius, weighted by the charge distribution as a:

$$a = \int_o^\infty r^2 4\pi r^2 \rho(r) dr \tag{22}$$

$$= 4\pi \int_o^\infty r^4 \rho(r) dr \tag{23}$$

Using this definition of the root-mean-square radius, it can be shown that for many useful spherically symmetric charge distributions, the Form Factor can be written as an expansion:

$$F(qa) = 1 - (\frac{q^2 a^2}{6}) + \cdots \tag{24}$$

This approximation to the form factor holds as long as the quantity qa remains small. This result is not entirely unexpected. For low energy collisions (small qa), we do not expect the electron to penetrate the nucleus and the scattering is goverend by the electromagnetic interaction. Therefore, all spherically symmetric charge distribution are going to appear similar from the outside. As a result, the scattering will be similar as well.

This point is emphasized by Figure 1, which is a plot of the (form factors)^2 vs (qa)^2. The details of the specified charge distributions can be found in Hofstadter's 1956 review paper (Rev. Mod. Phys. 28, 214 – 254 [1956]). They include Uniform, Gaussian, Exponential, Yukawa and other potentials.

4 Spatial Charge Distributions

We have shown that, in principle, a measured differential cross section can yield the Form Factor, $F(q)$. As what pointed out earlier, the Form Factor is simply the Fourier transform of the spatial charge distribution. So, if the Form Factor is known, the inverse Fourier transform will result in an expression for the spatial charge distribution. Therefore, taking measurements in the laboratory of the differential cross section of electrons scattered off a finite target can yield the spatial charge distribution of the target!

$$\rho(\vec{r}) \propto \int F(\vec{q}) e^{\frac{i\vec{q}\cdot\vec{r}'}{\hbar}} d^3\vec{q} \tag{25}$$

Figure 1: The square of the Form Factor vs $(qa)^2$ for several commonly used and useful spherically symmetric charge distributions

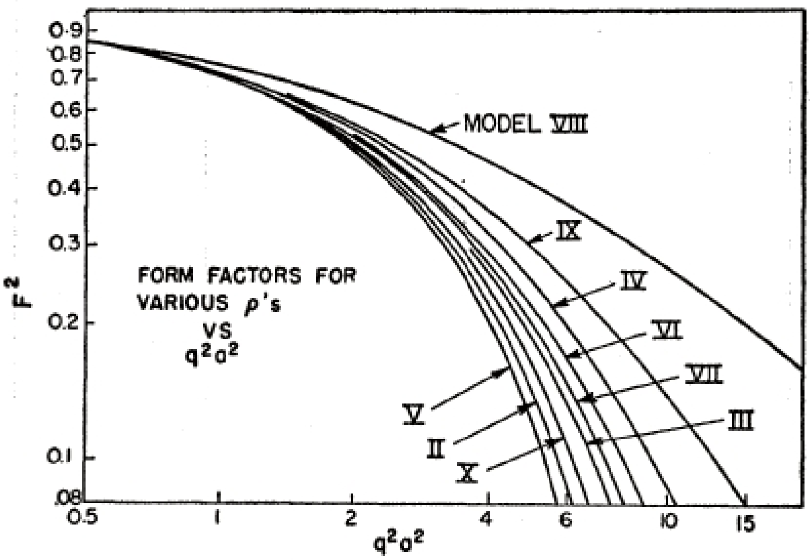

It should be noted that in order to explicitly invert the Form Factor using the Fourier transform, a complete measure of $\frac{d\sigma}{d\Omega}$ is required. In practice this is a very difficult measurement to take. Especially at large deflection angles (high momentum transfer collisions) it is difficult to accurately measure the differential cross section. As a result, fits and approximations are often used to fill in the missing data and perfom the inverse transform.

In the case of the spherically symmetric assumption, the resulting charge distribution is known as the Fermi model. Mathematically, the Fermi model is defined as:

$$\rho(r) = \frac{\rho_1}{exp\left[(r-c)/z_1\right]+1} \tag{26}$$

Figure 2 is a general picture of the Fermi model as presented by Hofstadter in his 1961 Nobel lecture. Of note, the Fermi model has two parameters which can be used to describe its shape. The first parameter is c, which can be seen as the radius of the charge distribution at 50% of the charge density. The second parameter is t, which is known as the 'skin thickness' and is defined by the radial distance between the point of 90% charge density and 10% charge density.

Figure 2: Fermi model of the gold nucleus, as presented by Hofstadter in 1961. The model is characterized by two parameters, the 'mean' radius c, and the skin thickness t.

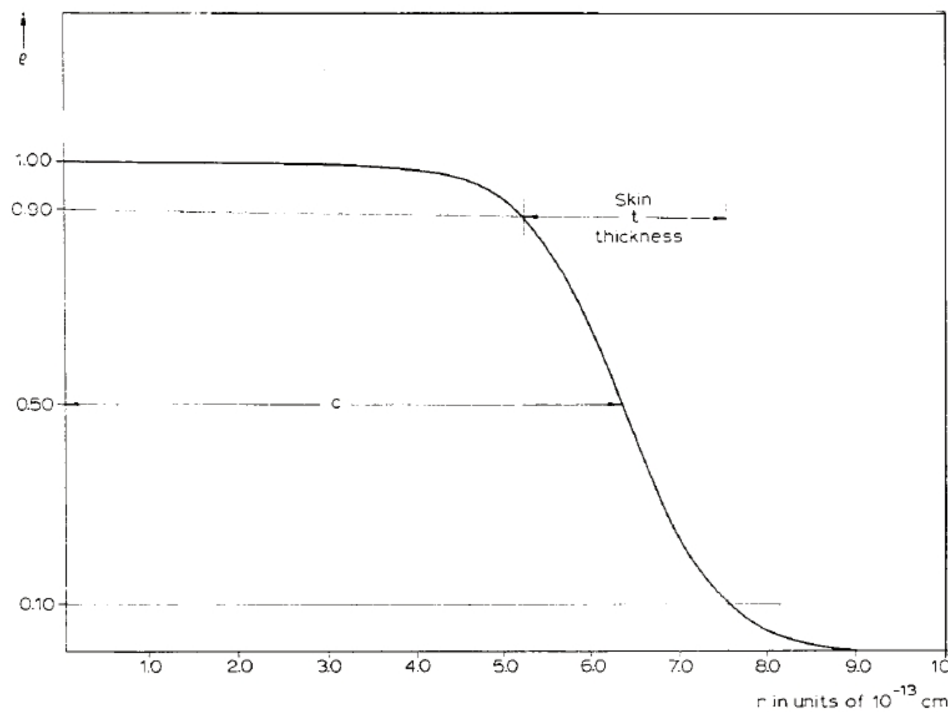

After performing electron scattering experiments using many different elemental nuclei as scattering targets, it became clear that there were an approximate relations that could be used to describe the parameters of these spherical nuclei. The relation for the radius parameter c was determined as:

$$c = (1.07 \pm 0.02)10^{-13} A^{\frac{1}{3}}\, cm \tag{27}$$

This relation is in agreement with the earlier estimates for the size of the nucleus as obtained by Rutherford and others. The relation for the skin thickness parameter t was determined as:

$$t = (2.4 \pm 0.3)10^{-13}\, cm \tag{28}$$

Which is simply a constant. This relation clearly holds for most light nuclei but should only be regarded as an approximation. Figure 3 (also presented by Hofstadter in 1961) gives a summary of approximate charge density distributions for various nuclei as determined using electron scattering experiments. Of note to this plot is that fact that the central charge densities of the various nuclei do not very much. There seems to be a tradeoff in the radius of the nuclei and the amount of charge contained therein.

It can also be seen that for elements with atomic mass equal and above that of calcium, the skin thickness parameter is essentially constant.

Finally it should be pointed out that Hydrogen and Helium are the obvious exceptions to the general ruels described above. In the case of the Hydrogen atom, the nucleus is simply a proton and so much higher charge density is to be expected.

5 Inelastic Scattering and Nuclear Structure

Up to this point we have been considering the case of elastic scattering, but it bears noting that inelastic scattering can also offer valuable information about the nuclear structure of the scattering target.

During an inelastic scattering event, the electron will deposit some extra energy in the target in the form of a nuclear excitation. By measuring the energy of the electrons after scattering, it is possible to discern some of the atomic structure. Figure 4 is a plot of scattered electron intensity vs. electron energy. The elastic scattering peak is clearly visible around 185 MeV(shifted down slightly from the original beam energy due to target recoil), while some of the inelastic scattering peaks are also visible at lower energies. This technique is best used to identify peaks with sufficiently different energy levels (limited by the energy resolution of your detector), as discerning between elastic and inelastic peaks can be difficult.

Figure 3: Summary of approximate charge density distributions for various nuclei as presented by Hofstadter in 1961.

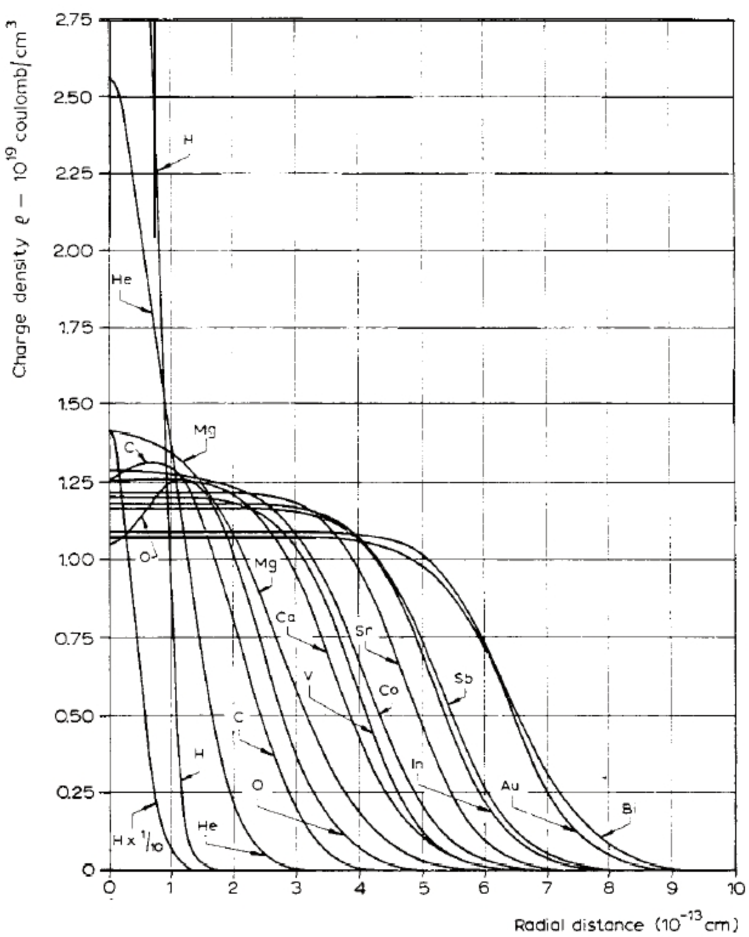

Figure 4: A plot of electron intensity vs. scattered electron energy of 187 MeV electrons scattered off a carbon-12 target. Note the distinct peaks with energy differences corresponding to the energies associated with excited states of the target.